IFSCC 2025 full paper (IFSCC2025-342)

"Hyaluronic Acid and Ectoine Inhibit Cutibacterium acnes Biofilm Formation and Reduce Skin Inflammation and Damage"

Yijie Liu [1,*], Yue Wu [1], Fan Chen[1], Yuqing Hu[1] and Dailin Xu[1]

[1]*In Vitro* Research Department, Bloomage Biotechnology Corporation Limited, Shanghai, China.

---

1. Introduction

Acne vulgaris, a multifactorial inflammatory disorder of the pilosebaceous unit, affects 85% of adolescents globally [1]. *Cutibacterium acnes (C.acnes*), a key pathogen in acne pathogenesis, employs biofilm-mediated virulence strategies and secretes lipases/cytotoxins to induce inflammatory cascades characterized by TNF-α/IL-1α overexpression [2-6]. These biofilms exhibit 10-1000× increased antibiotic resistance compared to planktonic counterparts, serving as reservoirs for chronic infection and medical device colonization [7-9]. Conventional therapies targeting microbial proliferation have been used extensively, however there is growing recognition of their limitations, which include the induction of erythromycin resistance in >60% of cases, disruption of commensal microbiota, and the inability to penetrate biofilms. This highlights the urgent need for innovative therapeutic strategies [10-12].

Emerging phytotherapeutic approaches demonstrate potential through distinct mechanisms: Sophorolipids have been shown to destabilise β-glucan matrices via steric hindrance, Myrtus communis extracts have been demonstrated to downregulate virulence genes by 60-95%, and oregano essential oil nanoemulsions have been observed to outperform clindamycin in biofilm eradication [13-16]. However, these monotherapeutic approaches are inadequate in addressing the tripartite pathogenesis of acne, namely the persistence of biofilms, dysregulated inflammation, and sebaceous dyshomeostasis.

Our study bridges this gap by leveraging the synergistic interaction between hyaluronic acid (HA) and extremolyte Ectoine (ECT), which uniquely destabilizes biofilm extracellular polymeric substances (EPS) through charge-mediated matrix remodeling. This complex concurrently regulates cytokine networks (IL-6/TNF-α/IL-1α) and restores skin barrier integrity

via morphology normalization, while preserving commensal flora through anti-biofilm activity. By integrating dynamic 3D biofilm models, cytokine profiling, we advance a paradigm-shifting therapeutic strategy that reconciles evolutionary biology with contemporary microbiome science.

2. Materials and Methods

2.1 Materials

Sodium hyaluronate (HA) and Ectoine (ECT) are commercial products provided by Bloomage Biotechnology Co., Ltd.,. The human epidermal keratinocyte (HEKn) were provided by American Type Culture Collection. ECT-HA complex solution containing 1% sodium hyaluronate and 1% Ectoine.

2.2 Bacterial strains and culture conditions

C. acnes (ATCC 6919) was cultivated in supplemented Schaedler's medium (Sigma-Aldrich, USA). The inoculum was prepared in saline solution and adjusted according to the McFarland scale [17]. Then, dilutions were made to find the better concentration for the infections.

2.3 Biofilm assay

A biofilm assay was performed as described by Hamada et al [18]. *C. acnes* biofilm was prepared in a 96-well microplate (Corning, US). *C. acnes* was cultured at 37℃ under anaerobic conditions with Aneropack Kenki for 7 days in BHI glucose broth medium to which complex were added to a final concentration of 1% of HA and 1% of Ectoine. Sterile distilled water without ingredients was used as a control. After culturing for 7 days, wells were rinsed with phosphate-buffered saline (PBS, pH 7.0), and biofilm that had formed on the well-bottom surfaces were air-dried for 60 min. Dried biofilm was stained with 0.1% crystal violet solution for 10 min, and then the wells were rinsed with PBS to remove unbound crystal violet from the biofilm. The staining solution was washed off the biofilm by adding 0.2 mL of 99.5% ethanol per well. The staining solutions were diluted to 20% with 99.5% ethanol. The absorbance of the diluted staining solutions at 595 nm was measured to evaluate the amount of biofilm formed. The number of viable bacteria in the biofilm was determined by adding 0.2 mL of PBS to the biofilm after 60 min of air-drying. The biofilm was then detached by pipetting, suspended in PBS and inoculated onto agar plates to enumerate the colony-forming units.

2.4 Generation of epidermal skin equivalents (RES)

As previously mentioned [18-20], epidermal skin models were created. In summary, 24 well plates were seeded with 2×10^5 keratinocytes from a secondary culture using Epilife media on

a filter insert (diameter 6.5 mm; Costar; Corning). Three days post-seeding, the keratinocytes were exposed to air after the apical medium was aspirated, with only the filter insert remaining in contact with the medium. During the liquid cultivation stage, a 0.1% (wt%) HA (0.8 kDa) solution was added to the culture media until the air-liquid culture was finished. The media was replaced with keratinocyte medium devoid of penicillin and streptomycin prior to the introduction of bacteria. Seven-day air-exposed cultures were used for the experimentation.

2.5 RES infections

After 7 days of cultivation, the RES were infected with the microorganisms.Skin equivalents were incubated along with 50 µL of the bacterial suspension. After infection, incubation took place in an incubator at 32 ℃ with 5% CO2. Different groups were evaluated and microorganism loads 24h, to evaluate the histological alterations. Infection of epidermal skin equivalents by the bacterium.

2.6 RES Histology analysis

After 24 h incubation, the infected RES were snap frozen in embedding medium for cryotomy (Sakura, Japan) and sectioned into 5 µm slices in cryostat (Wetzlar, Germany) and analyzed by optical microscopy using hematoxylin-eosin staining. The morphologies were analyzed and the thickness of the layers were measured by the software Fiji-ImageJ [21]. For immunohistochemistry, sections were fixed, blocked, and incubated with anti-lorincrin and anti-involucrin antibodies (Abcam,USA), followed by DAPI staining and fluorescence imaging.

2.7 Enzyme-linked immunosorbent assay (ELISA)

The supernatant was collected after 24 h of incubation and centrifuged for 5 min at 1000 rpm. The TNF-α/IL-6/IL-1α ELISA Kit (Lianke,China) was then used to measure the amount of cytokine in the supernatant in accordance with the protocol. The RIPA buffer (Solarbio,USA) was used to extract all proteins from the cells. Quantification of the total protein content was done using a ThermoFisher Scientific BCA kit. The total protein content served as a reference for the quantity of TNF-α, IL-1α and IL6 secreted by each group.

2.8 Biofilm of C. acnes in RES detected by scanning electron microscopy

A biofilm testing platform was established using the RES *C. acnes* infection model. In the gas-liquid phase, 50 µL of *C. acnes* bacterial solution (diluted to OD600=0.3 with PBS containing the test sample, and the blank control group was PBS) was added to the surface of the tissue, and the model was treated for 72 hours. After obtaining the infection model, the model tissues were fixed with tissue fixative, and then the growth of the bacterial film on the tissue surface was observed using a scanning electron microscope (SEM).

2.9 CLSM detects biofilm structure and live and dead bacteria

The dyes for staining the biofilm used in the CLSM (Confocal Laser Scanning Microscopy) detection of the biofilm structure and the ratio of live and dead bacteria were prepared according to the instructions of the LIVE/DEAD "BacLight" Bacterial Viability Kit. The *C.acnes* biofilm solution treated with ECT-HA complex, and the supernatant was aspirated and discarded. 200 μl of the dye was added to each well, and the staining was carried out in the dark for 15 minutes. The cell slides were taken out and inverted onto the glass slides. The software attached to the CLSM system was used to reconstruct the three-dimensional structure of the biofilm and calculate the ratio of live bacteria to dead bacteria.

2.10 Statistical analysis

The Student's t-test was applied to acquire the p-values. Statistical significance was deemed at $p < 0.05$, with p-values denoted as: $^{**}p < 0.01$, $^{*}p < 0.05$. The values are calculated from a minimum of three replicates and expressed as mean ± SD.

3. Results

3.1 Effect of ECT-HA on C. acnes biofilm

After the *in vitro* model of *C. acnes* biofilm was successfully constructed and the samples in different groups were treated, both the viability value and the content of the biofilm formation in the ECT-HA group were significantly lower than those in the control group. One-way analysis of variance (ANOVA) showed that there were statistically significant differences in the biofilm viability ($P < 0.005$) and content ($P < 0.001$) between the groups. The test results were shown in Table 1.

Table 1. Effect of ECT-HA on biofilm formation viability and content of *C. acnes.*

Groups	Biofilm formation viability	Biofilm content
Control	2.668±0.24	1.401±0.07
ECT-HA	1.882±0.41	1.039±0.13

3.2 Effect of ECT-HA on C. acnes biofilm structure

The biofilm of *C. acnes*, after being treated by different test groups, was observed under the Confocal Laser Scanning Microscopy (CLSM). The results showed that the biofilm of the control group had an overall regular and dense three-dimensional structure resembling a green lawn. In contrast, the biofilm structure of the ECT-HA group was significantly damaged. It gradually became dominated by red fluorescence. The more severe the structural damage was, the more obvious the red fluorescence became (Figure 1).

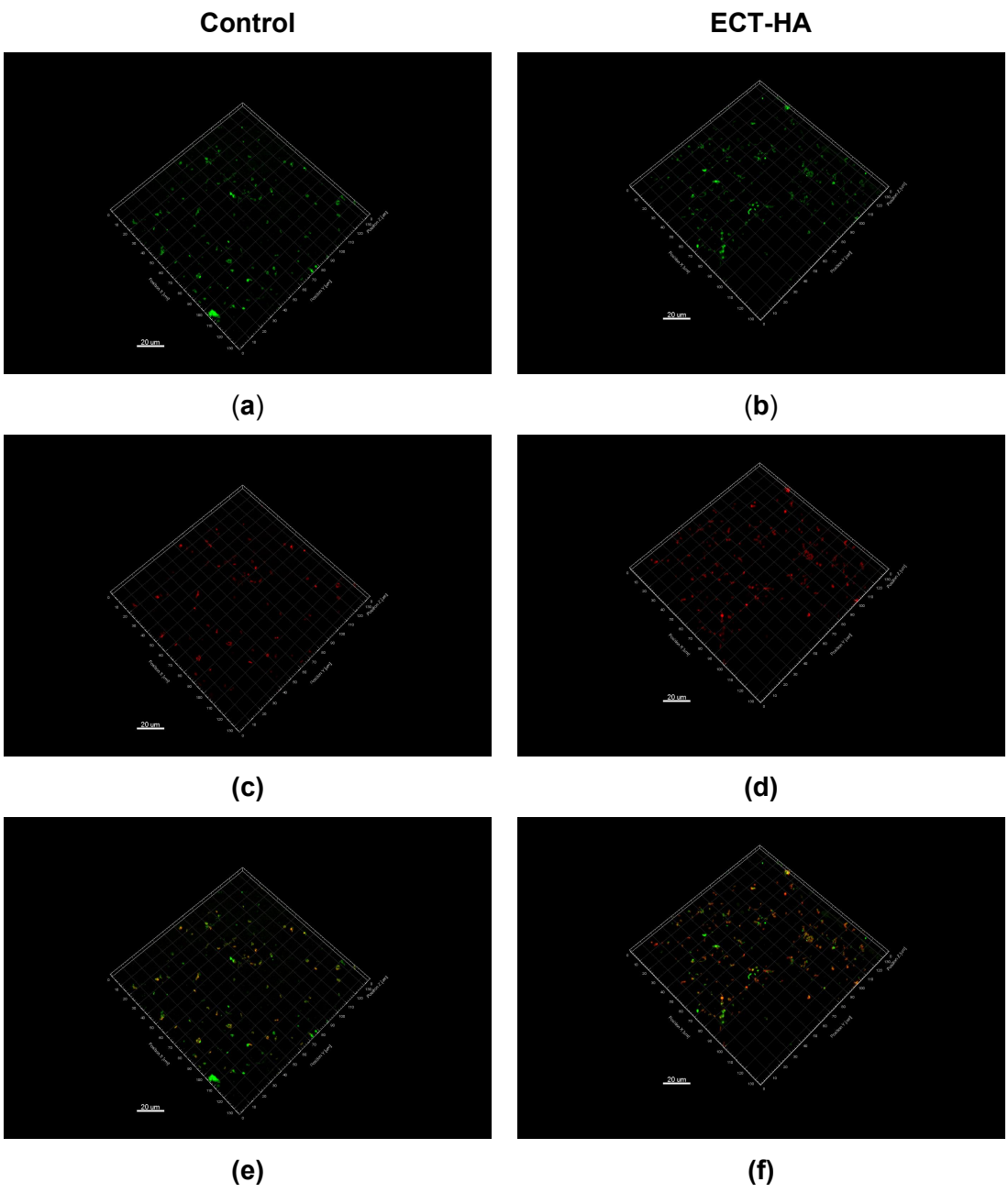

Figure 1 *C. acnes* LIVE/DEAD BacLight staining after treatment with ECT-HA observed under a fluorescence microscope. (a,c,e) Control untreated bacteria; (b,d,e) treated with ECT-HA.(a,b)Green fluorescent nucleic acid staining ;(c,d) Propidium iodide staining; (e,f) Merged.

3.3 Observation of Morphological Alternations of C. acnes Treated with ECT-HA

Visualization of the effect of ECT-HA on Biofilm Formation by Scanning Electron Microscopy (SEM). The SEM was chosen for analyzing the surface and morphological changes in biofilm cells exposed to ECT-HA. Regarding *C. acnes* biofilm formation, cellular adhesion and aggregation were detected in the untreated biofilm (control) (Figure 2a); however, for biofilm treated with ECT-HA, a lower number of adherent cells were observed (Figure 2b).

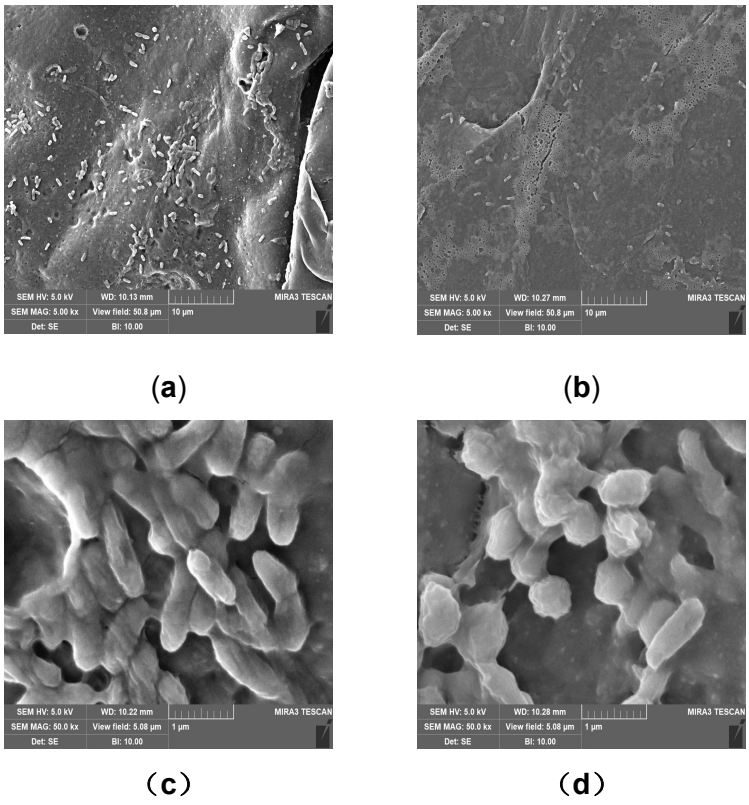

Figure 2 Scanning electron microscopy (SEM) of ECT-HA antibiofilm activity showing. (a) *C. acnes* untreated biofilm, (b) *C. acnes* biofilm treated with ECT-HA, (c) C.acnes biofilm treated with ECT-HA at a magnification. Notice the reduction in cellular adhesion of bacteria after treatment with ECT-HA.

3.4 ECT-HA Alleviate C.acnes Infection and Reduces the Secretion of Inflammatory Cytokines

Reconstructed epidermal skin equivalents (RES) are commonly employed for evaluating skincare or *in vitro* medicine efficacy due to their similar structure to human skin and resemblance to the in vivo environment. We created a *C.acnes* infection model of the skin to evaluate the efficacy of ECT-HA. Experiments on ECT-HA treated skin showed a more compact and continuous epidermal structure (Figure 3a-c). Immunofluorescence experiments on ECT-HA treated RES showed higher expression of barrier-associated proteins Lorincrin (Figure 3d-f) and Involucrin (Figure 3g-i). IL-6, IL-1α and TNF-α secretion was quantified by ELISA. The *C.acnes* stimulated group revealed significantly upregulated IL-6,IL-1α and TNF-α secretion (Figure 3c); in contrast, the ECT-HA treatment group exhibited down-regulated secretion of inflammatory cytokines. The levels of all cytokines (IL-6, IL-1α, and TNF-α) measured were very low or absent.

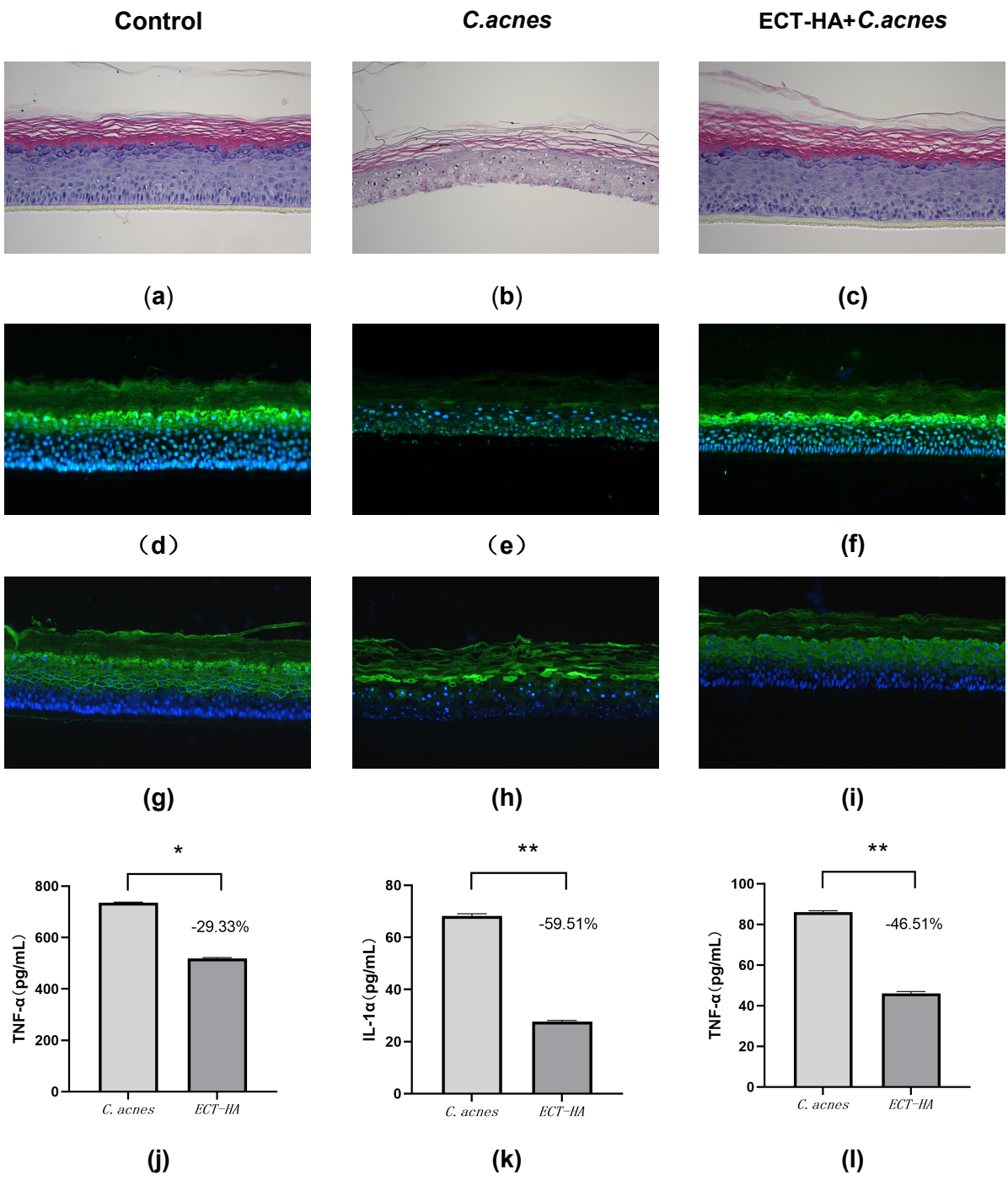

Figure 3 Effects of ECT-HA on tissue structure and pro-inflammatory cytokine production in *C. acnes*-stimulated RES. (a-c) Staining with H&E in equivalents of rebuilt epidermal skin. After the air-liquid phase, 50 μL of bacterial inoculum was added to insert to stimulate for 24 h for the *C.acnes* stimulation group; the experimental group was incubated for 24 h in advance with ECT-HA and then stimulated with *C.acnes* for 24 h. a: *C.acnes* untreated; b: *C.acnes* treated; c: treated with *C.acnes* and ECT-HA.(d-f) immunohistochemical analysis of Lorincrin expression variations in skin equivalents (ES) using DAPi(blue) and LOR (green) antibodies. Decreased LOR was observed in *C.acnes*-stimulated, ECT-HA-treated skin epidermal

equivalents; LOR accumulates in the stratum corneum. (g-i) immunohistochemical analysis of ivolucrin expression variations in RES using DAPi(blue) and IVL (green) antibodies. Decreased IVL was observed in *C.acnes*-stimulated, ECT-HA-treated skin epidermal equivalents; IVL accumulates in the stratum corneum. (j-l) The ECT-HA and *C.acnes* co-treated groups had reduced IL-6, IL-1α and TNF-α release, according to the enzyme-linked immunosorbent test (ELISA). The values are given as mean±SD. The unpaired t-test was used to determine P values. *Importance of the treated group compared to control group.

4. Discussion

The skin, as the outermost tissue of the human body, serves as a critical barrier against external pathogens and environmental stressors. However, pathogenic bacteria such as *Cutibacterium acnes* can form biofilms, significantly enhancing their drug resistance and virulence, thereby leading to persistent skin infections and inflammation. This study investigated the effects of a hyaluronic acid (HA) and Ectoine (ECT) complex on *C. acnes* biofilms and its impact on skin inflammation and barrier function using advanced in vitro models.

4.1 Effect of ECT-HA on C. acnes Biofilms

Biofilms formed by *C. acnes* are complex three-dimensional structures composed of extracellular polymeric substances (EPS), including polysaccharides, proteins, and extracellular DNA (eDNA). These structures confer significant antibiotic resistance and protect bacteria from host immune responses. Our results demonstrated that the ECT-HA complex effectively disrupts the three-dimensional architecture of *C. acnes* biofilms, reducing bacterial adhesion and aggregation while increasing the proportion of dead bacteria. This disruption is attributed to the charge-mediated matrix remodeling action of ECT-HA, which weakens the biofilm's structural integrity. Compared to conventional therapies, the ECT-HA complex shows promise in enhancing antibiotic efficacy by penetrating biofilms and reducing bacterial load.

4.2 Anti-inflammatory Effects of ECT-HA

C. acnes induces an inflammatory response by secreting lipases and cytotoxins, leading to the overexpression of pro-inflammatory cytokines such as TNF-α, IL-6, and IL-1α. Our study revealed that the ECT-HA complex significantly downregulates the secretion of these cytokines in infected skin models. This anti-inflammatory effect is likely mediated by HA's ability to maintain skin hydration, thereby reducing barrier damage, and ECT's protective

effects against external stressors. Additionally, ECT-HA may modulate host immune responses, inhibiting excessive cytokine production and mitigating inflammation.

4.3 Protective Effects of ECT-HA on Skin Barrier Function

The integrity of the skin barrier is essential for preventing pathogen invasion and maintaining skin homeostasis. Our findings indicate that ECT-HA treatment enhances the expression of barrier-associated proteins Lorincrin and Involucrin, resulting in a more compact and continuous epidermal structure. This suggests that ECT-HA not only strengthens the skin barrier but also promotes its repair, reducing the risk of secondary infections and inflammation.

4.4 Limitations and Future Directions

While our *in vitro* results are promising, the clinical efficacy of the ECT-HA complex remains to be validated *in vivo*. Future research should include clinical trials to assess its real-world application potential. Furthermore, exploring the molecular mechanisms underlying ECT-HA's action, particularly its effects on biofilm disruption and immune modulation, will be crucial for optimizing its therapeutic use.

5. Conclusion

This study systematically evaluated the effects of the hyaluronic acid (HA) and Ectoine (ECT) complex on *Cutibacterium acnes* biofilms and its impact on skin inflammation and barrier function using in vitro experiments and reconstructed epidermal skin models. The results showed that the ECT-HA complex could significantly disrupt the three-dimensional structure of *C. acnes* biofilms, reduce bacterial adhesion and aggregation, and lower the secretion of inflammatory cytokines while protecting the integrity of the skin barrier. These findings provide a scientific basis for developing novel anti-acne strategies and offer potential innovative solutions for the field of skin care. Future research will further explore the application effects of the ECT-HA complex in in vivo models and delve into its mechanisms of action to promote its widespread use in clinical and cosmetic applications.

References

[1] Yamazaki K, Akamatsu H, Oomori R,et al. Acne vulgaris and rosacea treatment guidelines. 2023. Nichihikaishi 133:407-450.

[2] Noguchi N. Antimicrobial resistance and infection control for gram-positive bacteria. 2021. Yakugaku Zasshi 141:235-244.

[3] Ebersole JL, Peyyala R, Gonzalez OA. Biofilm-induced profiles of immune response gene expression by oral epithelial cells. Mol Oral Microbiol. 2019.34(1):10.

[4] Fournière M, Latire T, Souak D, et al. *Staphylococcus epidermidis* and *Cutibacterium acnes:* Two Major Sentinels of Skin Microbiota and the Influence of Cosmetics. Microorganisms. 2020. 8(11):1752.

[5] Dessinioti C, Katsambas A. *Propionibacterium acnes* and antimicrobial resistance in acne. Clin. Dermatol. 2017, 35: 163-167.

[6] Han R, Blencke HM, Cheng H, et al. The antimicrobial effect of CEN1HC-Br against *Propionibacterium acnes* and its therapeutic and anti-inflammatory effects on acne vulgaris. Peptides. 2018, 99:36-43.

[7] Rather MA, Gupta K, Mandal M. Microbial biofilm: formation, architecture, antibiotic resistance, and control strategies. Braz J Microbiol. 2021,52(4):1701-1718.

[8] Hall CW, Mah TF. Molecular mechanisms of biofilm-based antibiotic resistance and tolerance in pathogenic bacteria. FEMS Microbiol Rev. 2017,41(3):276-301.

[9] de la Fuente-Nunez C, Cesaro A, et al. Antibiotic failure: Beyond antimicrobial resistance. Drug Resist Updat. 2023,71:101012.

[10] Bowler P, Murphy C, Wolcott R. Biofilm exacerbates antibiotic resistance: Is this a current oversight in antimicrobial stewardship. Antimicrob Resist Infect Control. 2020,9(1):162.

[11] Ding D, Wang B, Zhang X, et al. The spread of antibiotic resistance to humans and potential protection strategies. Ecotoxicol Environ Saf. 2023,254:114734.

[12] Larsson DGJ, Flach CF. Antibiotic resistance in the environment. Nat Rev Microbiol. 2022,20(5):257-269.

[13] Kaga H, Orita M, Endo K, et al. Interaction between Sophorolipids and β-glucan in Aqueous Solutions. J Oleo Sci. 2024,73(2):169-176.

[14] Dell'Annunziata F, Cometa S, Della Marca R, et al. *In Vitro* Antibacterial and Anti-Inflammatory Activity of Arctostaphylos uva-ursi Leaf Extract against *Cutibacterium acnes*. Pharmaceutics. 2022,14(9):1952.

[15] Taleb MH, Abdeltawab NF, Shamma RN, et al. Origanum vulgare L. Essential Oil as a Potential Anti-Acne Topical Nanoemulsion-*In Vitro* and *In Vivo* Study. Molecules. 2018;23(9):2164.

[16] Mias C, Chansard N, Maitre M, et al. Myrtus communis and Celastrol enriched plant cell culture extracts control together the pivotal role of *Cutibacterium acnes* and inflammatory pathways in acne. J Eur Acad Dermatol Venereol. 2023,37 Suppl 2:12-19.

[17] Meloni M, Balzaretti S, Collard N,et al. Reproducing the scalp microbiota community: co-colonization of a 3D reconstructed human epidermis with *C. acnes* and *M. restricta.* Int J Cosmet Sci. 2021,43(2):235–45.

[18] El Ghalbzouri A, Siamari R, Willemze R, et al. Leiden reconstructed human epidermal model as a tool for the evaluation of the skin corrosion and irritation potential according to the ECVAM guidelines. Toxicol. *In Vitro*. 2008,22:1311-1320.

[19]Thakoersing VS, Gooris GS, Mulder A, et al. Unraveling barrier properties of three different in-house human skin equivalents . Tissue Eng Part C Methods. 2012,18(1):1-11.

[20] Küchler S, Strüver K, Friess W. Reconstructed skin models as emerging tools for drug absorption studies. Expert Opin Drug Metab Toxicol. 2013,9(10):1255–63.

[21] Sanyal P, Paul S, Das A. Performance of a machine learning model in recognition of normal tissue from histological sections. Sci Rep. 2022,12(1):16420.